

Interband coherence induced correction to Thouless pumping: Possible observation in cold-atom systems

Gudapati Naresh Raghava, Longwen Zhou,* and Jiangbin Gong[†]

Department of Physics, National University of Singapore, Singapore 117546

Abstract

In Thouless pump, the charge transport in a one-dimensional insulator over an adiabatic cycle is topologically quantized. For nonequilibrium initial states, however, interband coherence will induce a previously unknown contribution to Thouless pumping. Though not geometric in nature, this contribution is independent of the time scale of the pumping protocol. In this work, we perform a detailed analysis of our previous finding [Phys. Rev. B **91**, 085420 (2015)] in an already available cold-atom setup. We show that initial states with interband coherence can be obtained via a quench of the system's Hamiltonian. Adiabatic pumping in the post-quench system are then examined both theoretically and numerically, in which the interband coherence is shown to play an important role and can hence be observed experimentally. By choosing adiabatic protocols with different switching-on speeds, we also show that the contribution of interband coherence to adiabatic pumping can be tuned. It is further proposed that the interband coherence induced correction to Thouless pumping may be useful in capturing a topological phase transition point. All our results have direct experimental interests.

PACS numbers: 03.65.Vf, 05.60.Gg, 05.30.Rt, 73.20.At

* zhoulw13@u.nus.edu

† phygj@nus.edu.sg

I. INTRODUCTION

Topological states of matter have attracted tremendous interests in the past decades [1, 2]. A large class of phases and phase transitions have been classified by topological invariants [1–4]. One such example is the quantum Hall effect, in which the robust quantization of Hall conductance originates from the topological Chern number of energy bands [5]. Other examples include topological insulators, topological superconductors, Weyl semimetals, etc. In recent years, analogue topological states in photonics, phononics and even acoustics have also been realized [6–8].

Most of the above mentioned topological phases are in equilibrium. In 1983, Thouless proposed a dynamical version of quantum Hall effect [9]. At zero temperature, he showed that the pumped charge through a one-dimensional insulator in an adiabatic cycle is quantized, with the contribution from each energy band (understood as a function of the quasimomentum and time) equal to their respective Chern numbers. At nonzero temperatures, the pumped charge will instead be given by an integral over Berry curvature weighted by initial populations of occupied bands. This is an early example in which geometric and topological quantities are introduced to describe quantum dynamics. This piece of rather fundamental physics, now termed Thouless pump, has been demonstrated recently in two cold-atom experiments [10, 11].

In the original proposal of Thouless pump, the initial state is assumed to be in thermal equilibrium. This is in clear contrast with recently discovered Floquet topological phases, which are intrinsically out-of-equilibrium [12–32]. Moreover, there have been increasing interests in exploring nonequilibrium response of topological states through quantum quench [33–50]. In this situation, the initial state will also be out-of-equilibrium, coherently populating several energy bands of the post-quench Hamiltonian. These new developments motivated us to generalize Thouless pump to situations in which nonequilibrium initial states are prepared.

In our previous work, we developed an adiabatic perturbation theory for periodically driven quantum systems [51]. Using the theory, we showed that the Thouless charge pump resulting from a non-equilibrium initial state has two components: a weighted integral of Floquet band Berry curvature, plus a correction due to interband coherence in the initial state [51]. So long as the pumping is in the adiabatic regime, the later component is

independent of the actual time scale of pumping and can be controlled extensively via choosing different adiabatic protocols. Later, such coherence induced correction to adiabatic pumping was found to exist in non-driven systems as well [52], even when the system is subject to dephasing.

In this work, taking advantage of two available cold-atom experiments reported very recently [10, 11], we show that by suddenly quenching the cold-atom Hamiltonian realized in the experiments, we can clearly generate the interband coherence effect in Thouless pump. In Sec. II, we introduce the already realized time-dependent Rice-Mele model and summarize the key results of our theory. In Sec. III, we propose to prepare initial states with interband coherence from Gaussian wave packets through quantum quench. The resulting states are then adiabatically pumped in parameter domains corresponding to different topological phases. We find that interband coherence plays an important role in the post-quenching pumping and thus may help us to dynamically detect and distinguish different topological phases. In Sec. IV, we further test interband coherence effects by adiabatic pumping of Wannier states after a quantum quench. In addition to leaving clear signatures around phase transition points, interband coherence effects are also shown to be manipulable via varying pumping protocols and even time durations (beyond the adiabatic regime), which suggests potential applications in quantum control tasks. In Sec. V, we summarize our results and discuss potential future directions.

II. RICE-MELE MODEL AND GENERALIZED THOULESS PUMP

The Rice-Mele model describes a double well lattice in one dimension [53]. Each of its unit cells has two sites separated by a staggered onsite potential. Recently, a dynamically modulated Rice-Mele model has been realized experimentally [10, 11]. The essential feature of this system can be described by the following tight-binding Hamiltonian:

$$\hat{H} = \sum_{n=1}^{L-1} \{ [J + \delta(t)(-1)^n] c_n^\dagger c_{n+1} + \text{h.c.} \} + \Delta(t) \sum_{n=1}^L (-1)^n c_n^\dagger c_n, \quad (1)$$

where n is the lattice site index, and L is the length of the lattice. The distance between each pair of adjacent lattice sites has been chosen to be 1. Both $\delta(t) = \delta_0 \cos(2\pi t/T)$ and $\Delta(t) = \Delta_0 \sin(2\pi t/T)$ are periodic functions of time t . Thus the tunneling amplitudes $J \pm \delta(t)$ and energy offset $\Delta(t)$ between adjacent lattice sites are periodically modulated in time. In

momentum space, the system is described by the Hamiltonian $\hat{H}(t) = \sum_k |k\rangle\langle k|h(k, t)$, with

$$H(k, t) = \{J + \delta(t) + [J - \delta(t)] \cos(k)\} \sigma_x - [J - \delta(t)] \sin(k) \sigma_y + \Delta(t) \sigma_z. \quad (2)$$

Here σ_x, σ_y and σ_z are three Pauli matrices. $k \in [-\pi, \pi)$ is the quasimomentum along x -direction. The sign of the parameter combination $J\delta_0\Delta_0$ controls phase transitions in the system. The spectrum of $H(k, t)$ becomes gapless when $J\delta_0\Delta_0 = 0$. When $2\pi t/T$ is viewed as a quasimomentum along a synthetic dimension, the Hamiltonian $H(k, t)$ is mapped onto a two-dimensional lattice model (also called the Harper-Hofstadter model) [54, 55], describing the minimum realization of a Chern insulator. At half-filling, this model is topologically nontrivial with band Chern numbers ± 1 . Thus the Hamiltonian $H(k, t)$ can also be interpreted as a dynamical realization of the Harper-Hofstadter model in a one-dimensional lattice, and the quantized Thouless pump observed there is determined by the Chern number of the two-dimensional parent model.

Experimentally, Thouless pump is observed by measuring the shift of a wave packet center over an adiabatic cycle [10, 11]. To observe quantized pumping, the initial state is assumed to uniformly fill the valence band, realizing a Wannier state in the lattice. However, under more general experimental conditions, the initial state could be out-of-equilibrium and coherently populates both the valence and conduction bands. Then how will the interband coherence in the initial state affect Thouless pump? In our recent studies, we found that for nonequilibrium initial states with k -reflection-symmetric populations, the Thouless pump is not quantized [51, 52]. This generalized Thouless pump contains two components, an integral over the geometric Berry curvature weighted by initial band populations, plus an accumulated dynamical effect due to interband coherence in the initial state. The shift of wave packet center over an adiabatic cycle is then given by [56]

$$\Delta\langle x \rangle = \Delta\langle x \rangle_1 + \Delta\langle x \rangle_2, \quad (3)$$

$$\Delta\langle x \rangle_1 = \frac{1}{2\pi} \sum_n \int_{-\pi}^{\pi} dk \int_0^{2\pi} d\beta B_{n,k}(\beta) \rho_{n,k}(0), \quad (4)$$

$$\Delta\langle x \rangle_2 = -\frac{1}{\pi} \sum_{m,n,m \neq n} \int_{-\pi}^{\pi} dk \text{Re} [C_{m,k}(0) C_{n,k}^*(0) W_{nm,k}(0)] \int_0^1 ds \frac{\partial E_{n,k}(s)}{\partial k}. \quad (5)$$

where m, n are energy band indices. $s \equiv t/T \in [0, 1)$ is the scaled time, $\beta = \beta(s)$ describes the adiabatic protocol (e.g., $\beta = 2\pi s$ for a linear protocol). In Eq. (4), $\rho_{n,k}(0)$ is the initial

population of the n th energy band at quasimomentum k . The Berry curvature $B_{n,k}(\beta)$ is defined as

$$B_{n,k}(\beta) \equiv i \left[\left\langle \frac{\partial \psi_{n,k}(\beta)}{\partial \beta} \middle| \frac{\partial \psi_{n,k}(\beta)}{\partial k} \right\rangle - \left\langle \frac{\partial \psi_{n,k}(\beta)}{\partial k} \middle| \frac{\partial \psi_{n,k}(\beta)}{\partial \beta} \right\rangle \right], \quad (6)$$

where $|\psi_{n,k}(\beta)\rangle$ is an instantaneous eigenstate of $H(k, \beta)$ with energy $E_{n,k}(\beta)$. In Eq. (5), $C_{n,k}(0)$ is the probability amplitude in Bloch basis $|\psi_{n,k}(0)\rangle$, and thus the cross term $C_{m,k}(0)C_{n,k}^*(0)$ with $m \neq n$ captures the interband coherence in the initial state. The other function $W_{nm,k}(0)$, also related to initial state coherence, is defined as

$$W_{nm,k}(0) \equiv \frac{\langle \psi_{n,k}(\beta) | \frac{\partial}{\partial \beta} | \psi_{m,k}(\beta) \rangle d\beta}{i [E_{m,k}(\beta) - E_{n,k}(\beta)] ds} \Big|_{s=0}. \quad (7)$$

This quantity is sensitive to the switching-on speed $\frac{d\beta}{ds}|_{s=0}$ of an adiabatic protocol. Moreover, it also has singular behaviors around band touching points, and thus would be important around topological phase transitions. Though the component $\Delta\langle x \rangle_1$ is already known in Thouless's original proposal, the contribution of $\Delta\langle x \rangle_2$ to adiabatic transport is only discovered recently in Ref. [51]. This correction term is intriguing because it is induced purely by interband coherence and it is independent of the time duration T of an adiabatic protocol. Thus it is highly valuable to experimentally observe this. In the following sections, we will motivate such type of experiments by studying how the coherence effects affect the pumping with different kinds of specific initial states and adiabatic protocols.

III. ADIABATIC PUMPING OF GAUSSIAN STATES AFTER QUENCH

Quantum quench provides with us a general approach to prepare a state with interband coherence. By starting with a state occupying only a single band, and quenching one of the Hamiltonian's parameter to another value, the state will coherently populate both the valence and conduction bands of the post-quench Hamiltonian. The adiabatic pumping of such a nonequilibrium initial state constitutes a generalized Thouless pump, in which the geometric nature of adiabatic states and accumulated non-adiabatic effects along a pumping path over a long time duration are both important.

In this section, to study the effect of interband coherence in adiabatic pumping, we propose to initialize the state of our system (i.e., the time-dependent Rice-Mele model discussed in the last section) with a Gaussian wave packet on the lattice. In the lattice

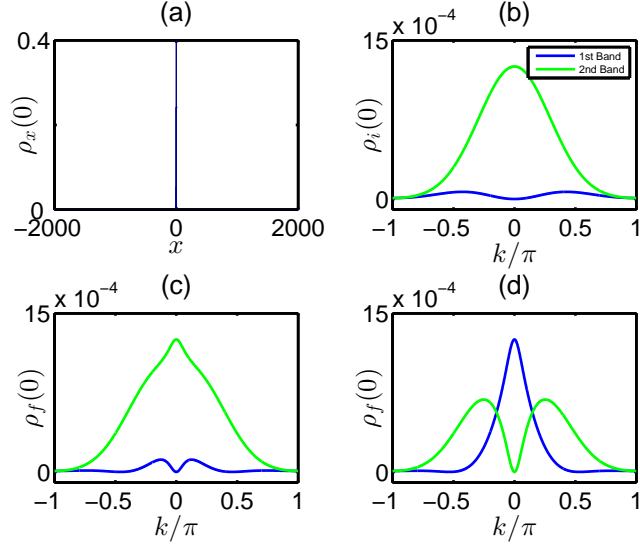


FIG. 1. (Color online) (a) Profile of the Gaussian wave function in the position space and (b) Probability distribution $\rho_i(0)$ on two bands along k for the Gaussian state before quenching at system parameters $\delta(0) = 0.85$, $\Delta(0) = 0$ and $J = 0$. (c) Probability distribution $\rho_f(0)$ on two bands along k of the Gaussian state after quenching the system parameter in the same topological phase. The final system parameter is $J_f = 0.1$. (d) Probability distribution $\rho_f(0)$ of the Gaussian state after quenching the system parameter across phase transition to $J_f = -0.1$.

representation, the profile of the wave packet is given by $Ae^{-(x-L/2)^2/d^2}$, where A is the normalization constant. In our simulation, we choose $L = 4000$ and $d = 20$. Such a parameter choice is to ensure that the wave packet has a relatively broad distribution in the momentum space, in order to capture interband coherence effects efficiently. The other parameters for the pre-quench system are chosen as $\delta(0) = 0.85$, $\Delta(0) = 0$ and $J = 1$, closing to the range of parameter values that can be realized experimentally [10]. The probability distributions of the Gaussian wave packet before the quench are shown in Figs. 1 (a) and 1 (b). We see that in momentum space, the Gaussian wave packet mainly populates the conduction band.

To introduce interband coherence into the initial state, we quench the system parameter J suddenly from $J = 1$ to different values $J = J_f \in [-1, 1]$. In the basis of the post-quench Hamiltonian, the Gaussian wave packet occupies both the conduction and valence bands at different values of k . In Figs. 1 (c) and 1 (d), we showed the probability distribution

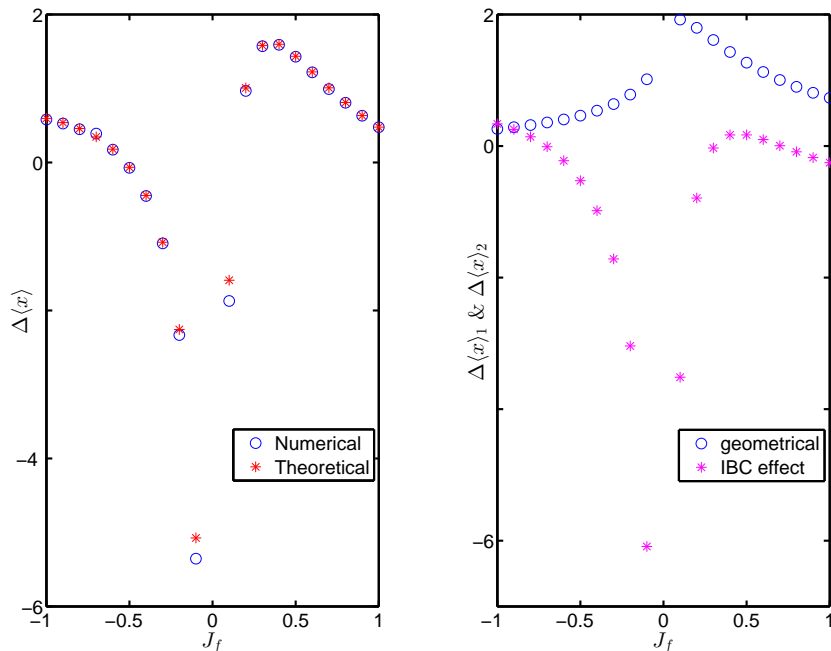


FIG. 2. (Color online) (a) Position expectation value after adiabatically pumping the Gaussian state besides quenching the system parameter to J_f . The numerical values (blue circles) are in agreement with theoretical values (red stars) except at the small window around the topological phase transition point, i.e., $J_f = 0$. The time duration of the linear pumping protocol is $T = 1000$. (b) The contribution of geometric and interband coherence (IBC) parts to the change of position expectation value, $\Delta\langle x \rangle_1$ and $\Delta\langle x \rangle_2$, after quenching and adiabatically pumping the Gaussian state.

$\rho_f(0)$ of the initial state in the basis of the post-quench Hamiltonian in two typical cases. In Fig. 1 (c), we set $J_f = 0.1$. Therefore the post-quench and pre-quench Hamiltonians belong to the same topological phase. In Fig. 1 (d), we choose $J_f = -0.1$, and thus the post-quench Hamiltonian belongs to a different topological phase as compared with the pre-quench Hamiltonian. Under such a quench, the initial population of the two bands at $k = 0$ get reversed. We give an analytical explanation of this observation in Appendix.

Once an initial state with interband coherence is prepared, we can pump it across the lattice under a given adiabatic protocol $\beta(s)$. The adiabatic limit corresponds to taking the time duration $T \rightarrow \infty$. In Fig. 2, we showed the shift of the center of post-quench

wave packets at different values of J_f over an adiabatic cycle, under a linear protocol $\beta(s) = 2\pi s$. In Fig. 2 (a), The numerical results (in blue circles) obtained from direct evolution of Schrodinger equation is compared with the theoretical predictions (in red stars) of Eq. (3). A good match is observed even if the post-quench Hamiltonian has a very small gap (i.e., around $J_f = 0$). Moreover, in Fig. 2 (b) we showed the contribution of weighted Berry curvature $\Delta\langle x \rangle_1$ and interband coherence $\Delta\langle x \rangle_2$ to the shift of wave packet center $\Delta\langle x \rangle$ separately. We observe that over the whole parameter domain J_f of the post-quench Hamiltonian, the pumping is dominated by the contribution of interband coherence in $\Delta\langle x \rangle_2$. Especially, $\Delta\langle x \rangle_2$ is peaked at $J_f = 0$, where the system undergoes a topological phase transition. So we conclude that interband coherence in a nonequilibrium initial state could not only play an important role in adiabatic transport, but also be a powerful tool to detect topological phase transitions dynamically. In the next section, we will further elaborate on these points and highlight some other intriguing features of interband coherence in adiabatic dynamics.

IV. ADIABATIC PUMPING OF WANNIER STATES AFTER QUENCH

In this section, we study adiabatic pumping of a Wannier state after a quantum quench. Before the quench, the Wannier state is prepared by superposing Bloch states uniformly across the valence band of the pre-quench Hamiltonian at $J = 1$. Such kind of states have been effectively prepared in recent cold atom experiments [10, 11]. After the sudden quench, the Wannier state populates both the conduction and valence bands of the post-quench Hamiltonian at $J = J_f$ coherently. Starting with such an initial state, we study how the contribution of interband coherence to adiabatic pumping will be affected by selecting adiabatic protocols with different switching-on speeds and time durations.

First, we explore the switching-on behavior of the adiabatic driving field by considering three different protocols: (i) $\beta_L = 2\pi s$, with a switching-on speed 2π , (ii) $\beta_S = 2\pi \sin\left(\frac{\pi s}{2}\right)$, with a switching-on speed π^2 , and (iii) $\beta_C = 2\pi[1 - \cos(\pi s)]$, with a switching-on speed 0. Based on our theoretical prediction in Eq. (5), the protocol β_S has a larger switching-on speed, and thus introducing larger interband coherence effects to adiabatic pumping than the other two protocols. Note also that the protocol β_C has a vanishing switching-on speed, thus suppressing the contribution of interband coherence in adiabatic pumping. In Fig. 3,

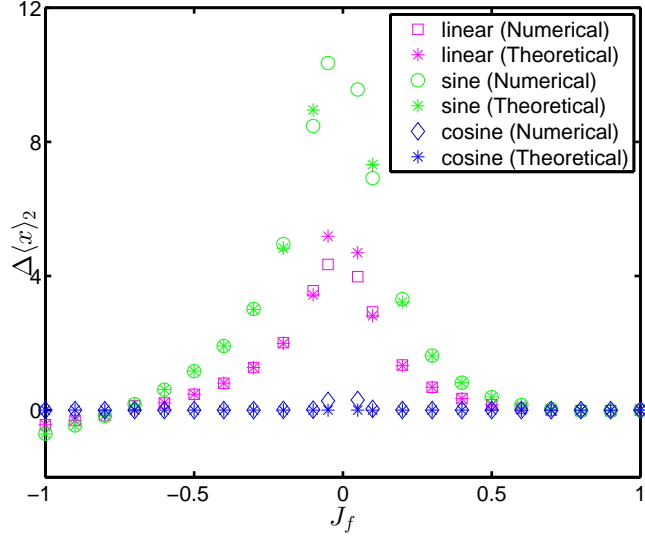


FIG. 3. (Color online) The contribution of interband coherence to the shift of Wannier state under different pumping protocols. Before the quench, the Wannier state was prepared at $J = 1$, occupying the lower band. The state was adiabatically pumped after quenching the system parameter to J_f . Interband coherence effect $\Delta\langle x \rangle_2$, from Eq. (5), is shown for three different pumping protocols: (i) $\beta_L = 2\pi s$, (ii) $\beta_S = 2\pi \sin(\frac{\pi s}{2})$, and (iii) $\beta_C = 2\pi[1 - \cos(\pi s)]$, both numerically and theoretically for $T = 1000$. The β_S pumping protocol has a larger contribution of interband coherence effect compared to the other two protocols.

we compare our theoretical predictions with direct numerical simulations, and obtain nice agreement between theory and numerics. In particular, in experiments, the difference in pumping among the three different adiabatic protocols can be regarded as a clear signature of the above-mentioned coherence-induced correction. Similar to the pumping of a Gaussian state after quench, we also observed a peak in the interband coherence induced wave packet shift $\Delta\langle x \rangle_2$ around the topological phase transition point $J_f = 0$. Such a universal behavior beyond specific initial state preparations again highlights the possibility of using interband coherence as a tool to detect topological phase transitions. The sensitivity of interband coherence effects to pumping protocols also has potential quantum control applications in adiabatic processes.

Since the contribution of interband coherence to adiabatic pumping originates from the accumulation of dynamical effects over a long time duration, it is important to know whether

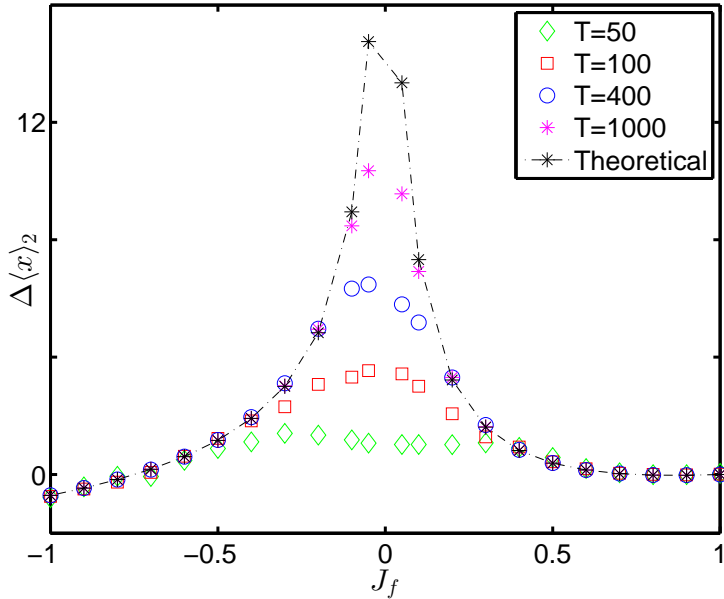


FIG. 4. (color online) Interband coherence effect for $\beta_S = 2\pi \sin\left(\frac{\pi s}{2}\right)$ pumping protocol with different time durations T . Before the quench, the system parameter $J = 1$. Interband coherence effects for pumping durations $T = 50$ (diamond), $T = 100$ (square), $T = 400$ (circle), and $T = 1000$ (star) are similar, except at the window around phase transition point.

and how will it be affected if the time duration of the adiabatic process is changed. Our theory indicates that it will be independent of T , but that is expected to be true only if the actual time duration of the pumping protocol is sufficiently long. Let us focus on the adiabatic protocol $\beta_S = 2\pi \sin\left(\frac{\pi s}{2}\right)$, and pump the initial state over adiabatic cycles with different time durations T . The results are shown in Fig. 4. We observe that the numerical simulations fit our theory quite well even for relatively small values of T , provided that the post-quench Hamiltonian is away from the gapless point $J_f = 0$. Close to $J_f = 0$, the gap of the post-quench Hamiltonian becomes small, and strong non-adiabatic effects appear in the dynamics. It is then anticipated that our theoretical predictions will deviate from numerical results, since the former is derived under first order adiabatic approximations. However, for not-too-short pumping durations, the peak around the topological phase transition point is still well-captured by the contribution from interband coherence. Thus we conclude that for nonequilibrium initial states, the interband coherence predicted by our theory can be observed even when the adiabatic protocol is not very slow. This observation is really good

news for possible experiments.

V. SUMMARY AND OUTLOOK

In this work, we performed detailed theoretical and numerical analysis on Thouless pump with nonequilibrium initial states, based on cold-atom experiments that are already available. It was shown that initial states with interband coherence can be prepared from Gaussian or Wannier states through quantum quenches. The change of position expectation value using such initial states (which can be measured in available experiments) during an adiabatic cycle is composed of two parts with different physical origins. Though both components converge to finite values in the adiabatic limit, one of them comes from geometric Berry curvature of the energy band, while the other arises from the accumulation of interband coherence effects over a pumping cycle. The contribution of interband coherence to Thouless pump is sensitive to the switching-on behavior of an adiabatic protocol and the size of band gap, thus having potential applications in designing adiabatic control strategies and detecting topological phase transitions. It should be promising and feasible to verify our predictions using existing experimental setups for Thouless pump [10, 11]. Such experiments will be useful towards extensions of Thouless pump and a better understanding of quantum adiabatic transport.

ACKNOWLEDGMENTS

Naresh would like to thank Prof. Dario Poletti for helpful discussions. This work is supported by NRF Grant No. NRF-NRFI2017-04 (WBS No. R-144-000-378-q281) and by Singapore Ministry of Education Academic Research Fund Tier I (WBS No. R-144-000-353-112).

Appendix A: Population reversal at $k = 0$

In this appendix, we show that the population of Gaussian state at quasimomentum $k = 0$ is reversed if the pre-quench and post-quench Hamiltonians belong to different topological

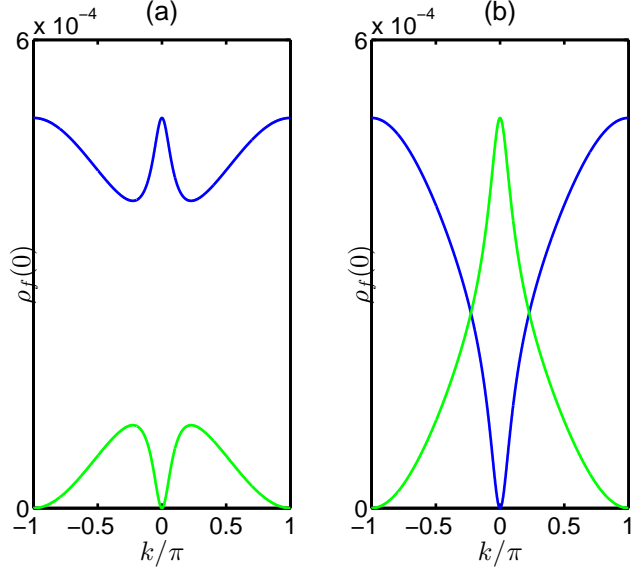


FIG. 5. (Color online) The initial system parameter $J = 1$ and $t = 0$ and topological phase transition occurs at the point $J = 0$. (a) $\rho_f(0)$ on two bands along k , after quenching the system to the same phase. The final system parameter $J_f = 0.1$. The probability distribution of the first band is exclusively populated at the value $k = 0$ as is the case before the quench. (b) $\rho_f(0)$ on two bands along k , after quenching the system to a different phase. The final system parameter $J_f = -0.1$. Note that the probability distribution of the second band is now exclusively populated at the value $k = 0$ which is in contrast to the case before the quench.

phases.

In momentum space, the Hamiltonian of Rice-Mele model is given by Eq. (2),

$$h(k, t) = \{J + \delta(t) + [J - \delta(t)] \cos(k)\} \sigma_x - [J - \delta(t)] \sin(k) \sigma_y + \Delta(t) \sigma_z.$$

The instantaneous energy spectrum $E(k, t)$ is then given by:

$$\begin{aligned} E(k, t) &= \sqrt{\Delta^2(t) + \{J + \delta(t) + [J - \delta(t)] \cos(k)\}^2 + [J - \delta(t)]^2 \sin^2(k)} \\ &= \pm \lambda \end{aligned} \tag{A1}$$

And the eigenvectors are,

$$|\psi_1\rangle = \frac{1}{\sqrt{\alpha^2 + \omega^2 + (\lambda + \beta)^2}} \begin{pmatrix} \alpha - i\omega \\ -\lambda - \beta \end{pmatrix} \quad (\text{A2})$$

$$|\psi_2\rangle = \frac{1}{\sqrt{\alpha^2 + \omega^2 + (\lambda - \beta)^2}} \begin{pmatrix} \alpha - i\omega \\ \lambda - \beta \end{pmatrix} \quad (\text{A3})$$

Here, $\alpha = J + \delta(t) + [J - \delta(t)] \cos(k)$, $\beta = \Delta(t)$, and $\omega = -[J - \delta(t)] \sin(k)$.

Let us now prepare our initial state $|\psi\rangle$ by populating only the first band in k -space at a particular value of $J = J_i$. Then we quench the state by changing the parameter J of the Hamiltonian to $J = J_f$.

The wave function in the pre-quench eigenbasis, is given as,

$$|\psi\rangle = |\psi_1\rangle_i \quad (\text{A4})$$

And in the post-quench eigenbasis it is given as,

$$|\psi\rangle = \eta_1 |\psi_1\rangle_f + \eta_2 |\psi_2\rangle_f \quad (\text{A5})$$

at each k . The two coefficients η_1 and η_2 are given by

$$\eta_1 = {}_f\langle\psi_1|\psi_1\rangle_i \quad (\text{A6})$$

$$\eta_2 = {}_f\langle\psi_2|\psi_1\rangle_i. \quad (\text{A7})$$

Note that α , ω and λ are all depend on the system parameter J . Using Eqs. (A2) and (A3), we obtain

$$\eta_1 = \frac{(\alpha_i - i\omega_i)(\alpha_f + i\omega_f) + (\lambda_i + \beta)(\lambda_f + \beta)}{\sqrt{\alpha_i^2 + \omega_i^2 + (\lambda_i + \beta)^2} \sqrt{\alpha_f^2 + \omega_f^2 + (\lambda_f + \beta)^2}} \quad (\text{A8})$$

$$\eta_2 = \frac{(\alpha_i - i\omega_i)(\alpha_f + i\omega_f) - (\lambda_i + \beta)(\lambda_f - \beta)}{\sqrt{\alpha_i^2 + \omega_i^2 + (\lambda_i + \beta)^2} \sqrt{\alpha_f^2 + \omega_f^2 + (\lambda_f - \beta)^2}} \quad (\text{A9})$$

For simplification, let us look at the particular value of $k = 0$ at $t = 0$, for different values of J . So, we have $\delta = \delta_0$, $\Delta = 0$, $\alpha = 2J$, $\beta = 0$, $\omega = 0$, $\lambda = |\alpha| = 2|J|$. Therefore, when the pre-quench and post-quench systems belong to the same topological phase, we have $J_i J_f > 0$. It implies that

$$\eta_1|_{k=0} = \frac{J_i J_f + J_i J_f}{\sqrt{J_i^2 + J_i^2} \sqrt{J_f^2 + J_f^2}} = 1. \quad (\text{A10})$$

So the population of the lower band is preserved at $k = 0$, as shown in Figure 5 (a). But if we quench our Hamiltonian to the other topological phase, we will have $J_i J_f < 0$. Then Eq. (A9) implies that

$$\eta_1|_{k=0} = \frac{J_i J_f - J_i J_f}{\sqrt{J_i^2 + J_i^2} \sqrt{J_f^2 + J_f^2}} = 0; \quad (\text{A11})$$

Therefore the population at $k = 0$ in the lower band is fully transferred to the higher band at the same k after the quench. The result is shown in Fig. 5 (b).

So we conclude that the population at $k = 0$ is reversed if the pre-quench and post-quench Hamiltonians belong to different topological phases.

-
- [1] M. Z. Hasan and C. L. Kane, *Colloquium: Topological insulators*, Rev. Mod. Phys. **82**, 3045 (2010).
 - [2] X. L. Qi and S. C. Zhang, *Topological insulators and superconductors*, Rev. Mod. Phys. **83**, 1057 (2011).
 - [3] S. Q. Shen, *Topological Insulators: Dirac Equation in Condensed Matters*, (Springer-Verlag, Berlin Heidelberg, 2012).
 - [4] C.-K. Chiu, J. C. Y. Teo, A. P. Schnyder, and S. Ryu, *Classification of topological quantum matter with symmetries*, Rev. Mod. Phys. **88**, 035005 (2016).
 - [5] D. J. Thouless, M. Kohmoto, M. P. Nightingale, and M. den Nijs, *Quantized Hall Conductance in a Two-Dimensional Periodic Potential*, Phys. Rev. Lett. **49**, 405 (1982).
 - [6] L. Lu, J. D. Joannopoulos, and M. Soljačić, *Topological states in photonic systems*, Nat. Phys. **12**, 626 (2016).

- [7] R. Süsstrunk and S. D. Huber, *Observation of phononic helical edge states in a mechanical topological insulator*, Science **349**, 47 (2015).
- [8] Z. Yang, F. Gao, X. Shi, X. Lin, Z. Gao, Y. Chong, and B. Zhang, *Topological Acoustics*, Phys. Rev. Lett. **114**, 114301 (2015).
- [9] D. J. Thouless, *Quantization of particle transport*, Phys. Rev. B **27**, 6083 (1983).
- [10] S. Nakajima, T. Tomita, S. Taie, T. Ichinose, H. Ozawa, L. Wang, M. Troyer, and Y. Takahashi, *Topological Thouless pumping of ultracold fermions*, Nat. Phys. **12**, 296 (2016).
- [11] M. Lohse, C. Schweizer, O. Zilberberg, M. Aidelsburger, and I. Bloch, *A Thouless quantum pump with ultracold bosonic atoms in an optical superlattice*, Nat. Phys. **12**, 350 (2016).
- [12] T. Oka and H. Aoki, *Photovoltaic Hall effect in graphene*, Phys. Rev. B **79**, 081406(R) (2009).
- [13] J.-I. Inoue and A. Tanaka, *Photoinduced Transition between Conventional and Topological Insulators in Two-Dimensional Electronic Systems*, Phys. Rev. Lett. **105**, 017401 (2010).
- [14] T. Kitagawa, E. Berg, M. S. Rudner, and E. Demler, *Topological characterization of periodically driven quantum systems*, Phys. Rev. B **82**, 235114 (2010).
- [15] N. H. Lindner, G. Refael, and V. Galitski, *Floquet topological insulator in semiconductor quantum wells*, Nat. Phys. **7**, 490 (2011).
- [16] L. Jiang, T. Kitagawa, J. Alicea, A. R. Akhmerov, D. Pekker, G. Refael, J. I. Cirac, E. Demler, M. D. Lukin, and P. Zoller, *Majorana Fermions in Equilibrium and in Driven Cold-Atom Quantum Wires*, Phys. Rev. Lett. **106**, 220402 (2011).
- [17] Z. Gu, H. A. Fertig, D. P. Arovas, and A. Auerbach, *Floquet Spectrum and Transport through an Irradiated Graphene Ribbon*, Phys. Rev. Lett. **107**, 216601 (2011).
- [18] B. Dóra, J. Cayssol, F. Simon, and R. Moessner, *Optically Engineering the Topological Properties of a Spin Hall Insulator*, Phys. Rev. Lett. **108**, 056602 (2012).
- [19] D. Y. H. Ho and J. B. Gong, *Quantized Adiabatic Transport In Momentum Space*, Phys. Rev. Lett. **109**, 010601 (2012).
- [20] Y. T. Katan and D. Podolsky, *Modulated Floquet Topological Insulators*, Phys. Rev. Lett. **110**, 016802 (2013).
- [21] Q.-J. Tong, J.-H. An, J. B. Gong, H.-G. Luo, and C. H. Oh, *Generating many Majorana modes via periodic driving: A superconductor model*, Phys. Rev. B **87**, 201109(R) (2013).
- [22] M. S. Rudner, N. H. Lindner, E. Berg, and M. Levin, *Anomalous Edge States and the Bulk-Edge Correspondence for Periodically Driven Two-Dimensional Systems*, Phys. Rev. X **3**,

- 031005 (2013).
- [23] L. Zhou, H. Wang, D. Y. H. Ho, and J. B. Gong, *Aspects of Floquet bands and topological phase transitions in a continuously driven superlattice*, Eur. Phys. J. B **87**, 204 (2014).
 - [24] G. Usaj, P. M. Perez-Piskunow, L. E. F. Foa Torres, and C. A. Balseiro, *Irradiated graphene as a tunable Floquet topological insulator*, Phys. Rev. B **90**, 115423 (2014).
 - [25] L. E. F. Foa Torres, P. M. Perez-Piskunow, C. A. Balseiro, and G. Usaj, *Multiterminal Conductance of a Floquet Topological Insulator*, Phys. Rev. Lett. **113**, 266801 (2014).
 - [26] D. Y. H. Ho and J. B. Gong, *Topological effects in chiral symmetric driven systems*, Phys. Rev. B **90**, 195419 (2014).
 - [27] M. Lababidi, I. I. Satija, and E. Zhao, *Counter-propagating Edge Modes and Topological Phases of a Kicked Quantum Hall System*, Phys. Rev. Lett. **112**, 026805 (2014).
 - [28] D. Carpentier, P. Delplace, M. Fruchart, and K. Gawedzki, *Topological Index for Periodically Driven Time-Reversal Invariant 2D Systems*, Phys. Rev. Lett. **114**, 106806 (2015).
 - [29] T. S. Xiong, J. B. Gong, and J. H. An, *Towards large-Chern-number topological phases by periodic quenching*, Phys. Rev. B **93**, 184306 (2016).
 - [30] R. W. Bomantara, G. N. Raghava, L. W. Zhou, and J. B. Gong, *Floquet topological semimetal phases of an extended kicked Harper model*, Phys. Rev. E **93**, 022209 (2016).
 - [31] P. Titum, E. Berg, M. S. Rudner, G. Refael, N. H. Lindner, *Anomalous Floquet-Anderson Insulator as a Nonadiabatic Quantized Charge Pump*, Phys. Rev. X **6**, 021013 (2016).
 - [32] S. Mukherjee, A. Spracklen, M. Valiente, E. Andersson, P. Öhberg, N. Goldman, and R. R. Thomson, *Experimental observation of anomalous topological edge modes in a slowly driven photonic lattice*, Nat. Commun. **8**, 13918 (2017).
 - [33] W. DeGottardi, D. Sen, and S. Vishveshwara, *Topological phases, Majorana modes and quench dynamics in a spin ladder system*, New J. Phys. **13**, 065028 (2011).
 - [34] M. S. Foster, M. Dzero, V. Gurarie, and E. A. Yuzbashyan, *Quantum quench in a $p + ip$ superfluid: Winding numbers and topological states far from equilibrium*, Phys. Rev. B **88**, 104511 (2013).
 - [35] P. D. Sacramento, *Fate of Majorana fermions and Chern numbers after a quantum quench*, Phys. Rev. E **90**, 032138 (2014).
 - [36] G. Kells, D. Sen, J. K. Slingerland, and S. Vishveshwara, *Topological blocking in quantum quench dynamics*, Phys. Rev. B **89**, 235130 (2014).

- [37] Y. Dong, L. Dong, M. Gong, and H. Pu, *Dynamical phases in quenched spin-orbit-coupled degenerate Fermi gas*, Nat. Commun. **6**, 6103 (2015).
- [38] L. D'Alessio and M. Rigol, *Dynamical preparation of Floquet Chern insulators*, Nat. Commun. **6**, 8336 (2015).
- [39] M. D. Caio, N. R. Cooper, and M. J. Bhaseen, *Quantum Quenches in Chern Insulators*, Phys. Rev. Lett. **115**, 236403 (2015).
- [40] P. Wang, W. Yi, and X. Gao, *Topological phase transition in the quench dynamics of a one-dimensional Fermi gas with spin-orbit coupling*, New J. Phys. **17**, 013029 (2015).
- [41] M. D. Caio, N. R. Cooper, and M. J. Bhaseen, *Hall response and edge current dynamics in Chern insulators out of equilibrium*, Phys. Rev. B **94**, 155104 (2016).
- [42] Y. Hu, P. Zoller, and J. C. Budich, *Dynamical Buildup of a Quantized Hall Response from Nontopological States*, Phys. Rev. Lett. **117**, 126803 (2016).
- [43] J. H. Wilson, J. C. W. Song, and G. Refael, *Remnant Geometric Hall Response in a Quantum Quench*, Phys. Rev. Lett. **117**, 235302 (2016).
- [44] F. N. Ünal, E. J. Mueller, and M. Ö. Oktel, *Nonequilibrium fractional Hall response after a topological quench*, Phys. Rev. A **94**, 053604 (2016).
- [45] P. D. Sacramento, *Edge mode dynamics of quenched topological wires*, Phys. Rev. E **93**, 062117 (2016).
- [46] Z. Huang, and A. V. Balatsky, *Dynamical Quantum Phase Transitions: Role of Topological Nodes in Wave Function Overlaps*, Phys. Rev. Lett. **117**, 086802 (2016).
- [47] A. G. Grushin, S. Roy, and M. Haque, *Response of fermions in Chern bands to spatially local quenches*, J. Stat. Mech. 083103, (2016).
- [48] P. Wang, and S. Kehrein, *Phase transitions in the diagonal ensemble of two-band Chern insulators*, New J. Phys. **18**, 053003, (2016).
- [49] C. Wang, P. Zhang, X. Chen, J. Yu, and H. Zhai, *Measuring Topological Number of a Chern-Insulator from Quench Dynamics*, arXiv:1611.03304 (2016).
- [50] U. Bhattacharya, J. Hutchinson, A. Dutta, *Quenching in Chern insulators with satellite Dirac points*, arXiv:1605.04768 (2016).
- [51] H. L. Wang, L. W. Zhou, and J. B. Gong, *Interband coherence induced correction to adiabatic pumping in periodically driven systems*, Phys. Rev. B **91**, 085420 (2015).
- [52] L. W. Zhou, D. Y. Tan, and J. B. Gong, *Effects of dephasing on quantum adiabatic pumping*

- with nonequilibrium initial states*, Phys. Rev. B **92**, 245409 (2015).
- [53] M. J. Rice and E. J. Mele, *Elementary Excitations of a Linearly Conjugated Diatomic Polymer*, Phys. Rev. Lett. **49**, 1455 (1982).
- [54] P. G. Harper, *Single band motion of conduction electrons in a uniform magnetic field*, Proc. Phys. Soc. London A **68**, 874 (1955).
- [55] D. R. Hofstadter, *Energy levels and wave functions of Bloch electrons in rational and irrational magnetic fields*, Phys. Rev. B **14**, 2239 (1976).
- [56] In theory, there is another correction term (often very small) to adiabatic pumping due to initial transient effects. However, this term does not build up as the number of cycles increases. In fact it is time independent. Therefore this term does not reflect quantum pumping and can be safely neglected [51].